

NATIONAL INSTITUTE FOR FUSION SCIENCE

Cross Section for Production of Excited Hydrogen Atoms Following Dissociative Excitation of Molecular Hydrogen by Electron Impact

T. Fujimoto, K. Sawada and K. Takahata

(Received – Sep. 8, 1989)

NIFS-DATA-4

Mar. 1990

RESEARCH REPORT NIFS-DATA Series

This report was prepared as a preprint of compilation of evaluated atomic, molecular, plasma-wall interaction, or nuclear data for fusion research, performed as a collaboration research of the Data and Planning Center, the National Institute for Fusion Science (NIFS) of Japan. This document is intended for future publication in a journal or data book after some rearrangements of its contents.

Inquiries about copyright and reproduction should be addressed to the Research Information Center, National Institute for Fusion Science, Nagoya 464-01, Japan.

**Cross Section for Production of Excited Hydrogen Atoms
Following Dissociative Excitation of Molecular Hydrogen
by Electron Impact**

T. Fujimoto, K. Sawada and K. Takahata

(Received – Sep. 8, 1989)

NIFS-DATA-4

Mar. 1990

CROSS SECTION FOR PRODUCTION OF EXCITED HYDROGEN ATOMS FOLLOWING DISSOCIATIVE
EXCITATION OF MOLECULAR HYDROGEN BY ELECTRON IMPACT

Takashi Fujimoto, Keiji Sawada and Kiyoto Takahata

*Department of Engineering Science, Faculty of Engineering, Kyoto University,
Kyoto 606, Japan*

Abstract

For the purpose of investigating molecular hydrogen present in plasmas, the production cross section of excited hydrogen atoms due to dissociative excitation of molecular hydrogen by electron collisions has been estimated from the emission cross sections of Lyman and Balmer lines.

Keywords: molecular hydrogen, dissociative excitation, electron collisions,
Balmer lines

I . INTRODUCTION

Hydrogen (deuterium) is the main constituent of fusion research plasmas, and inside the main plasma of a magnetic confinement scheme e.g., tokamak and helical machines, only atomic hydrogen and protons would be present besides impurities. In the outer region of the plasmas or in a divertor plasma, however, molecular hydrogen would also be present or its density may even dominate over atomic hydrogen density. Upon collisions by electrons these hydrogen molecules may emit atomic hydrogen lines as well as molecular bands. The former radiation is due to dissociative excitation of a hydrogen molecule, i.e., excitation to a repulsive excited molecular state followed by dissociation into an excited atomic state. Knowledge of the cross section for this process of emission of atomic lines is therefore needed for a study of molecular hydrogen present in these plasmas.

The cross section for emission of Lyman and Balmer lines due to dissociative excitation has been measured by several workers. The experimental set-up is such that a low pressure molecular hydrogen gas is bombarded by an electron beam, and atomic emission lines are observed from a direction at right angles to the direction of the beam. Thus, the emission cross section of the respective line is obtained.

We envisage a plasma having a finite n_e , so that we can assume a statistical population distribution among the different l sublevels of an excited state of the hydrogen atom. This situation differs substantially from the above experimental conditions under which the emission cross sections of Lyman or Balmer lines are measured for dissociative excitation of molecular hydrogen by electron collisions. For the calculation of the population distribution of excited atomic hydrogen we need the cross section for

excitation into a particular state which consists of sublevels with various l values. This cross section, which we shall call the production cross section, differs from the emission cross section for the Lyman or Balmer lines, the data on which are abundant.^{1,2} In the following section, we review the experimental data for the emission cross sections and estimate the production cross section.

II. PRODUCTION CROSS SECTION

In order to convert an emission cross section into a production cross section, we need to know the production cross section for each of the l sublevels, or the "branching ratio" of the production cross sections for the various l sublevels. Such information is quite scarce, except for the cross sections for the $p = 2, 3$ and 4 levels, where p denotes the principal quantum number. In the case of $p = 2$, the emission cross section for the Lyman α line and the production cross section for the $2s$ level have been measured separately.^{3,4} References 5 and 6 also give the Lyman α line emission cross section. By adopting the corrections proposed in refs. 6 and 7, we multiplied the cross section in refs. 3 and 5 by 0.8×0.69 and that in refs. 4 and 6 by 0.69 to obtain the appropriate emission cross section corrected for the sensitivity of the detector. These cross sections are shown in Fig. 1. We then added these emission cross sections^{3,4} to obtain the production cross section for the $p = 2$ atoms. Since the branching ratio of the cross sections for $2s$ and $2p$ are practically independent of energy for energy regions higher than 50 eV, we multiplied the Lyman α -line emission cross section^{5,6} by a factor of 1.48 , the inverse of the branching ratio. The result is shown in Fig. 1 by the large symbols.

For $p = 3$, the emission cross section for the Balmer α line^{3,8-14} is

known. The emission cross section for the Lyman β line was measured¹⁵ at 100 eV and the authors assumed its energy dependence to be the same as that for the Balmer α line.¹² Again, we multiplied the Lyman β cross section by 0.69. These cross sections are indicated in Fig. 2 by the small symbols and symbol \blacktriangledown . The branching ratio of the production cross sections has been determined for the 3s, 3p and 3d levels in the threshold region, using the technique of level anticrossing spectroscopy.¹⁶ This ratio is 6:54:41. Unfortunately, the branching ratio in the higher energy regions is not known, but is expected to be different from the low-energy value and is of present interest. To deduce it, we proceed as follows: From the Lyman β emission cross section we estimate the production cross section for the 3p level and hence the emission cross section for the 3p \rightarrow 2s transition, and we subtract the latter cross section from the emission cross section for the Balmer α line. The result is the production cross section for the 3s and 3d levels together. We have thus obtained the total production cross section of the $p = 3$ atoms by starting from the emission cross sections for the Lyman β and Balmer α lines. Following the assumption¹⁵ that the ratio of the two emission cross sections, namely 3p \rightarrow 2s and (3s \rightarrow 2p and 3d \rightarrow 2p), is independent of energy, we now multiply the emission cross section for the Balmer α line by a factor of 1.63, the inverse of the corresponding branching ratio. The result is shown in Fig. 2.

For $p = 4$ we have a branching ratio measurement in the high-energy range; by recording the time-evolution of the Balmer β fluorescence intensity following pulsed excitation and resolving the decay curve into three components, Ogawa et al.¹⁷ determined the relative emission cross sections for the 4s, 4p and 4d sublevels. These cross sections are easily converted into

production cross sections. At 100 eV, for example, the latter are 15 ± 3 , 49 ± 35 and 36 ± 5 for 4s, 4p and 4d, respectively. The authors found that the branching ratio depended only slightly on energy. Due to the short lifetime of the 4p state, the cross section for this state is subject to a large uncertainty. In order to estimate the production cross section summed over the various l sublevels, we made the following assumptions. First, the production cross section to the levels with $l \geq 3$ is zero. This assumption may be justified since, judging from the magnitudes of the emission cross section, the total angular momentum of the colliding system is not much larger than 1 and the production of an atom having $l \geq 3$ is quite unlikely. The second assumption is that the branching ratio for the s, p and d sublevels in this and higher-lying states is the same as for the 3s, 3p and 3d states. The latter branching ratio is determined by dividing the production cross section of (3s and 3d together) according to the branching ratio for 4s and 4d. The resulting branching ratio for 3s, 3p and 3d is 16:44:40. The production cross section for the $n = 4$ atoms is obtained from the emission cross section of the Balmer β line;^{3, 8-14} the latter is multiplied by 2.25. The resulting production cross section is indicated in Fig. 3 by the large symbols.

For the levels $p \geq 5$, the two above assumptions are also made. The production cross sections for $p = 5$ and 6 atoms are obtained from the emission cross sections for the Balmer γ and δ lines by multiplying them by 2.58 and 2.68, respectively. The result is shown in Figs. 4 and 5.

We have not corrected the emission cross section for cascading. According to ref. 3, the only emission cross section which includes a substantial cascade effect is that for Lyman α ; the cascade contribution is 10 % at 50 eV and 5 % at 1000 eV. This appears to be within the experimental uncertainties (See

Fig. 1) and justifies ignoring the effects of cascades.

Since, in the measurement of the emission cross section, the excitation by electron collisions is highly anisotropic, the excited atoms may be aligned and the emitted radiation may be polarized. (See Figs. 3 and 7 in ref. 18) However, in the case of the Balmer line emission the polarization is found to be very small³ and in the case of Lyman radiations, no experimental data is available. Therefore, for the present, we decided to neglect the effect of alignment of excited atoms. In the future it may be necessary to take this effect into account in estimating the production cross section.

The excitation threshold of the emission cross section is somewhat indefinite in the experiment. We are considering a plasma with an electron temperature T_e in the range of 10 - 100 eV, and at these high temperatures a small uncertainty in the threshold energy does not much affect the excitation rate coefficient. We arbitrarily assume the excitation threshold to be 17 eV, and we adopt the following expression for all the excited levels, which is an extension of the formula for the cross section in the Bethe-Born approximation as proposed in ref. 3.

$$\sigma = 4\pi a_0^2 R K [1 - s \exp(-rE)](\ln E + C)/E \quad (1)$$

where E is the energy of the electrons in eV, R is one Rydberg (13.6 eV) and K , s , r and C are adjustable parameters. The parameter K is derived from the originally determined parameter M^2 in refs. 3, 4 and 13, and C is given in refs. 4 and 13, both for all levels except $p \geq 6$. We fitted eq. (1) to our estimated production cross section by adjusting the parameters s , and r , as shown in Figs. 1 - 5. Table I shows the resulting values of the fitting

parameters. The rapid increase in C with an increase in p reflects the changes of the energy dependence of the production cross section as seen in Figs. 1 - 5.

Since there is no experimental information on the production cross sections for levels $p \geq 7$, we extrapolated the cross sections for $p \leq 6$ to higher levels by assuming a smooth variation. Table I shows the values of the parameters.

Figure 6 shows the dissociative excitation (production) rate coefficients calculated for several temperatures from the above cross sections in relation to the principal quantum number p . This figure also includes the excitation rate coefficient for atomic hydrogen, which is taken from our previous calculation.¹⁹ The two rate coefficients show significantly different p -dependences. Roughly speaking, the former is proportional to p^{-6} , while the latter is to p^{-3} , the p -dependence of the oscillator strengths of the Lyman lines.

References

1. H. Tawara, Y. Itikawa, Y. Itoh, T. Kato, H. Nishimura, S. Ohtani, H. Takagi, K. Takayanagi and M. Yoshino, Report IPPJ-AM-46 (Institute of Plasma Physics, Nagoya University, 1986).
2. H. Tawara, Y. Itikawa, H. Nishimura and M. Yoshino, Report IPPJ-AM-55 (Institute of Plasma Physics, Nagoya University, 1987).
3. D.A. Vroom and F.J. de Heer, *J. Chem Phys.* **50**, 580 (1969).
4. G.R. Möhlmann, K.H. Shima and F.J. de Heer, *Chem. Phys.* **28**, 331 (1978).
5. G.H. Dunn, R. Geballe and D. Pretzer, *Phys. Rev.* **128**, 2200 (1962).
6. M.J. Mumma and E.C. Zipf, *J. Chem. Phys.* **55**, 1661 (1971).
7. D.E. Shemansky, J.M. Ajello and D.T. Hall, *Astrophys. J.* **296**, 765 (1985).
8. E.R. Williams, J.V. Martinez and G.H. Dunn, *Bull. Am. Phys. Soc.* **12**, 233 (1967).
9. L.D. Weaver and R.H. Hughes, *J. Chem. Phys.* **52**, 2299 (1970).
10. R.S. Freund, J.A. Schiavone and D.F. Brader, *J. Chem. Phys.* **64**, 1122 (1976).
11. G.A. Khayrallah, *Phys. Rev. A* **13**, 1989 (1976).
12. C. Karolis and E. Harting, *J. Phys. B* **11**, 357 (1978).
13. G.R. Möhlmann, F.J. de Heer and J. Los, *Chem. Phys.* **25**, 103 (1977).
14. J.M. Kurepa, M.D. Tasic and Z.L. Petrovic, (private communication).
15. J.M. Ajello, D. Shemansky, T.L. Kwok and Y.L. Yung, *Phys. Rev. A* **29**, 636 (1984).
16. L. Julien, M. Glass-Maujean and J.P. Descoubes, *J. Phys. B* **6**, L196 (1973).
17. T. Ogawa, M. Taniguchi and K. Nakashima, Abstract of Contributed Papers (Fifteenth International Conference on the Physics of Electronic and Atomic Collisions, Brighton 1987) p.339.

18. T. Fujimoto, C. Goto, Y. Uetani and K. Fukuda, Jpn. J. Appl. Phys. **24**, 875 (1985).
19. T. Fujimoto, S. Miyachi, and K. Sawada, Nucl. Fusion **28**, 1255 (1988).

Table I

Parameter values in eq.(1), which are employed in this calculation.

p	K	s	r	C
2	0.146	1.081	0.01265	-1.249
3	6.63×10^{-3}	1.159	do.	2.152
4	6.95×10^{-4}	1.232	do.	11.50
5	1.20×10^{-4}	1.239	do.	27.09
≥ 6	$31.3 p^{-7.75}$	do.	do.	$69.86 \ln(0.295p)$

Figure Captions

Fig. 1. The emission cross section for the Lyman α radiation (upper small symbols denoted as "2p") and the production cross section for the 2s atoms (lower small symbols denoted as "2s"). Δ : ref. 3 (multiplied by 0.8 x 0.69). \circ : ref. 4 (multiplied by 0.69). \square : ref. 5 (multiplied by 0.8 x 0.69) and ref. 6 (multiplied by 0.69). The production cross section for the $p = 2$ atoms derived from these cross sections is shown by the large symbols. The solid curve represents a fit of the semiempirical formula, eq.(1), to the production cross section data.

Fig. 2. The emission cross section for the Balmer α line (small symbols denoted as "emis."). Δ : ref. 3. \diamond : ref. 8. \bullet : ref. 9. \blacklozenge : ref. 10 (relative measurement). \square : ref. 11. ∇ : ref. 12 (relative measurement). \circ : ref. 13. \blacktriangle : ref. 14. The emission cross section for the Lyman β line at 100 eV (\blacktriangledown : ref. 15.). Large symbols show the production cross section for the $p = 3$ atoms. The solid curve represents a fit of eq.(1) to the data points.

Fig. 3. The emission cross section for the Balmer β line (small symbols denoted as "emis.") and the production cross section for the $p = 4$ atoms (large symbols). The notations are the same as in Fig. 2. The curve represents a fit of eq.(1) to the data points.

Fig. 4. The emission cross section for the Balmer γ line (small symbols denoted as "emis.") and the production cross section for the $p = 5$ atoms (large symbols). The notations are the same as in Fig. 3. The curve

represents a fit of eq.(1) to the data points.

Fig. 5. The emission cross section for the Balmer δ line (small symbols denoted as "emis.") and the production cross section for the $p = 6$ atoms (large symbols). The notations are the same as in Fig. 3. The curve represents a fit of eq.(1) to the data points.

Fig. 6. Dependence of the rate coefficient for production of excited atoms from molecular hydrogen on the principal quantum number (open symbols). O: $T_e = 10$ eV, \square : 100 eV, and Δ : 1000 eV. The excitation rate coefficient from atomic hydrogen is also shown by the closed symbols. The lines show the slope of the function p^{-6} and of p^{-3} .

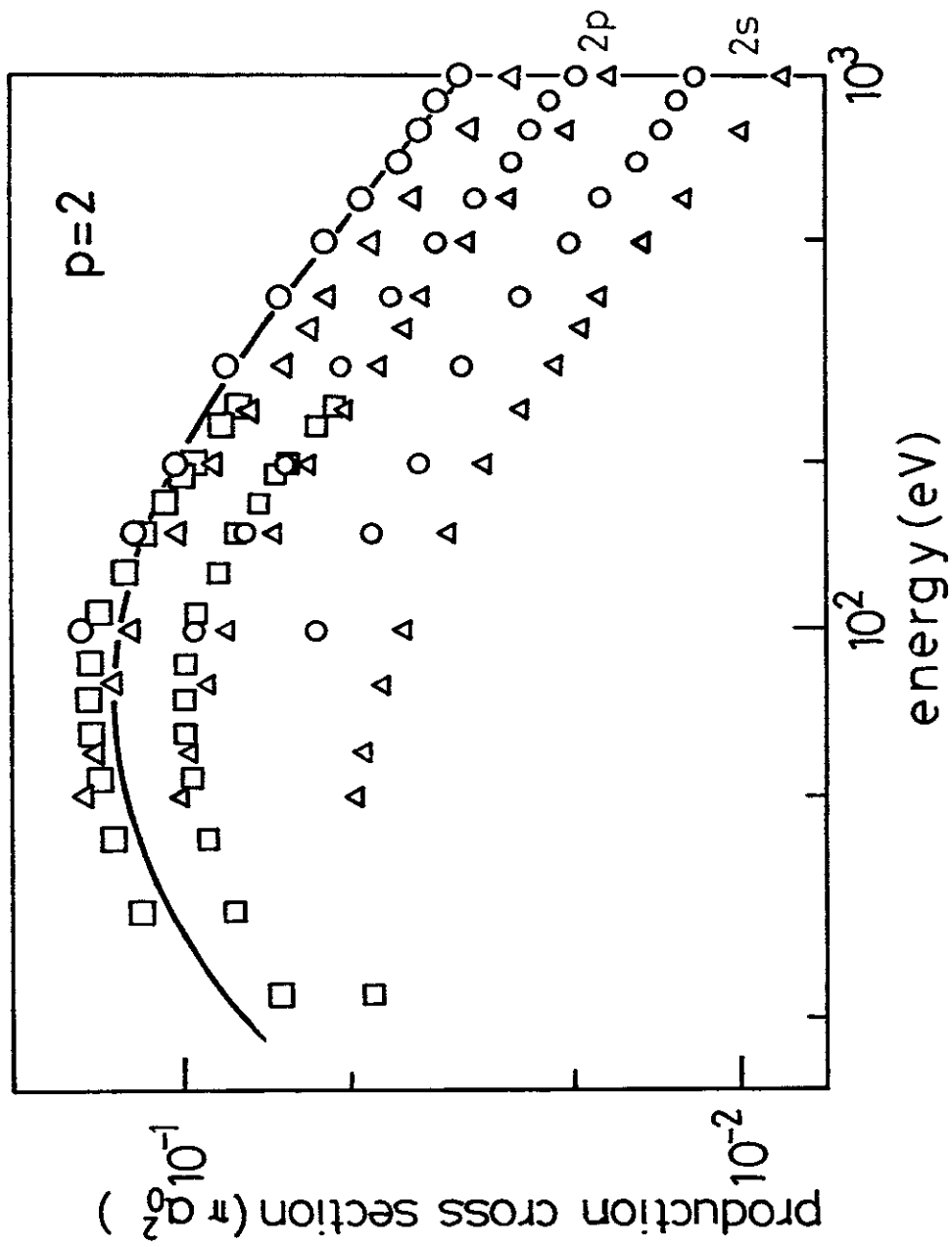


Fig. 1

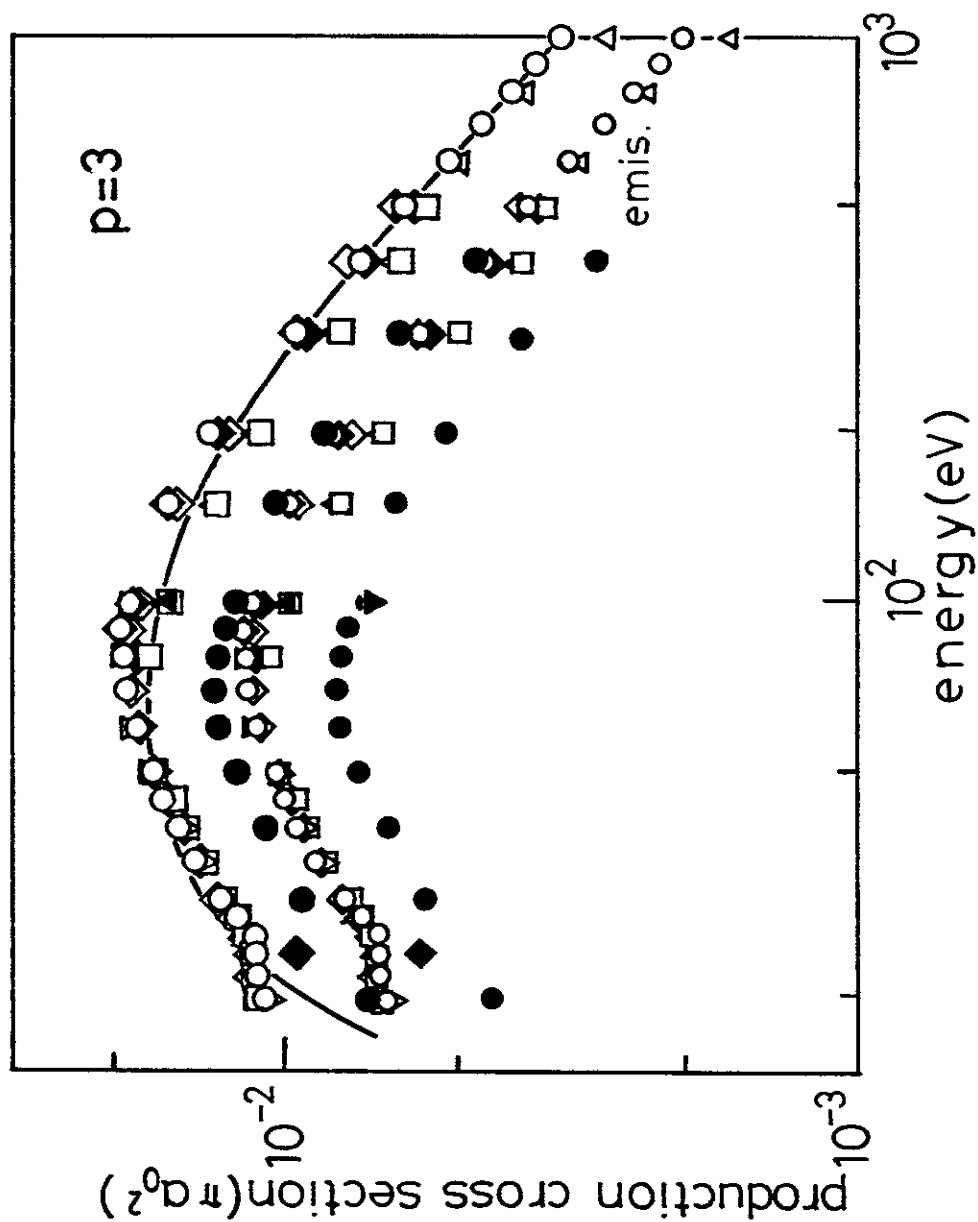


Fig. 2

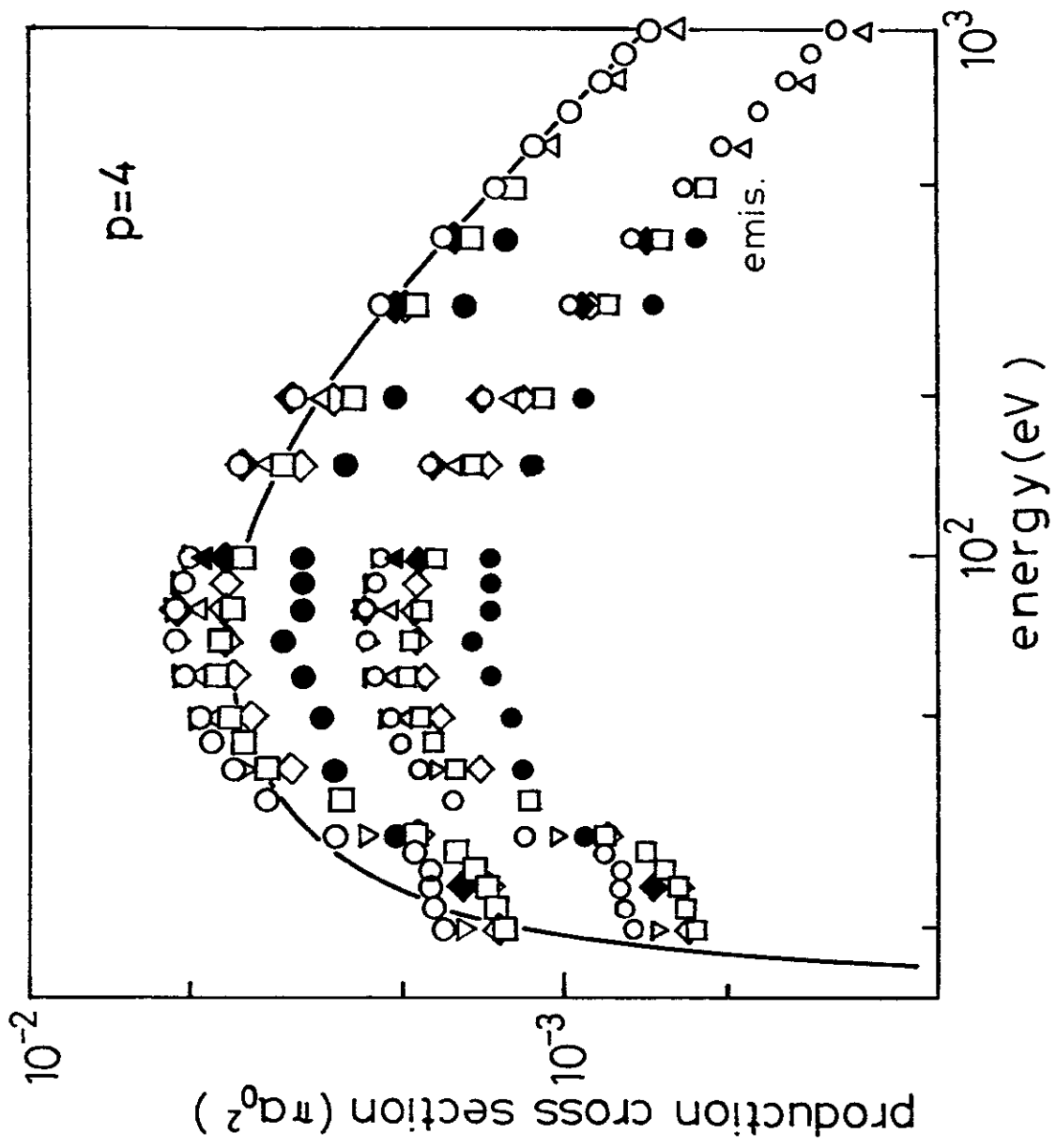


Fig. 3

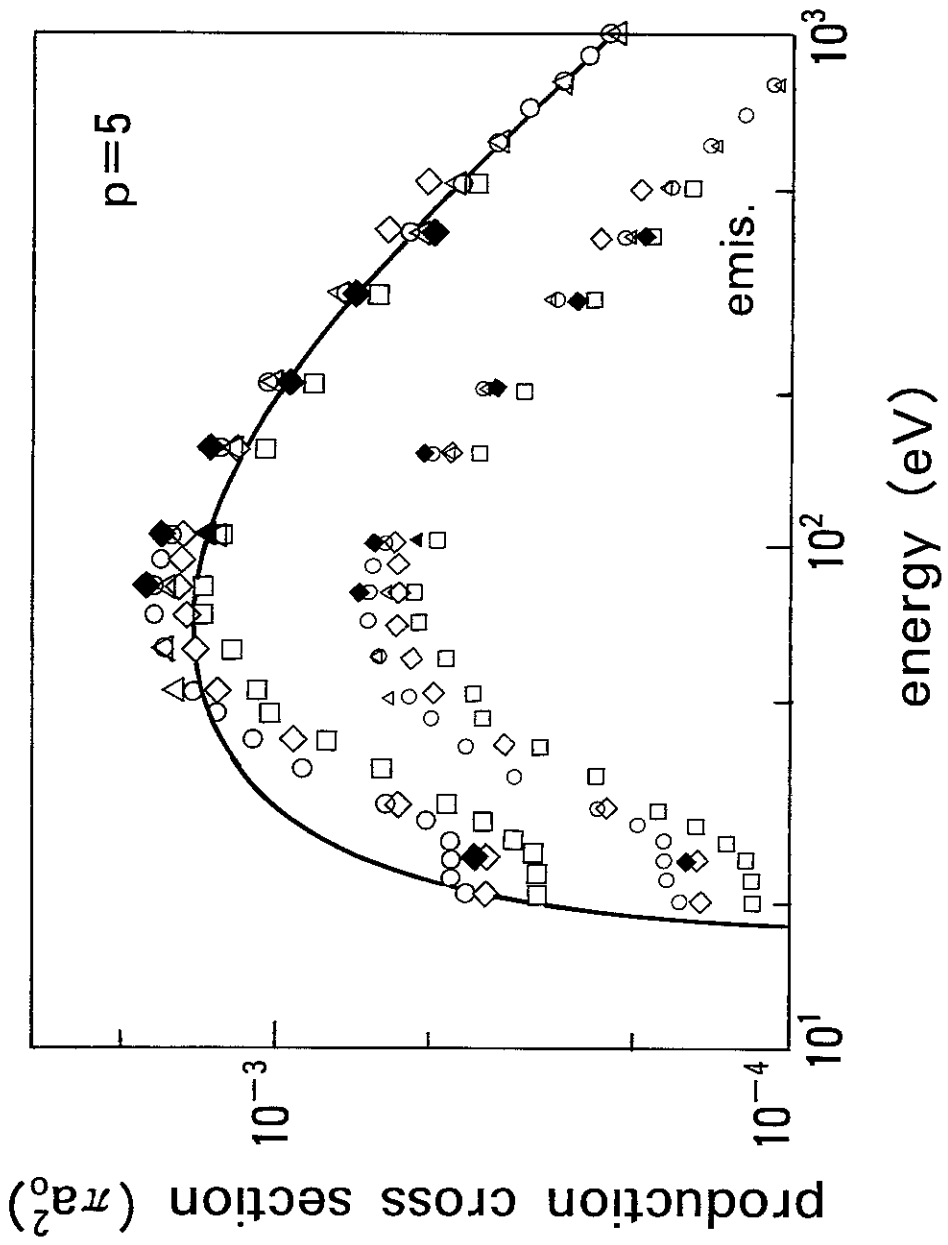


Fig. 4

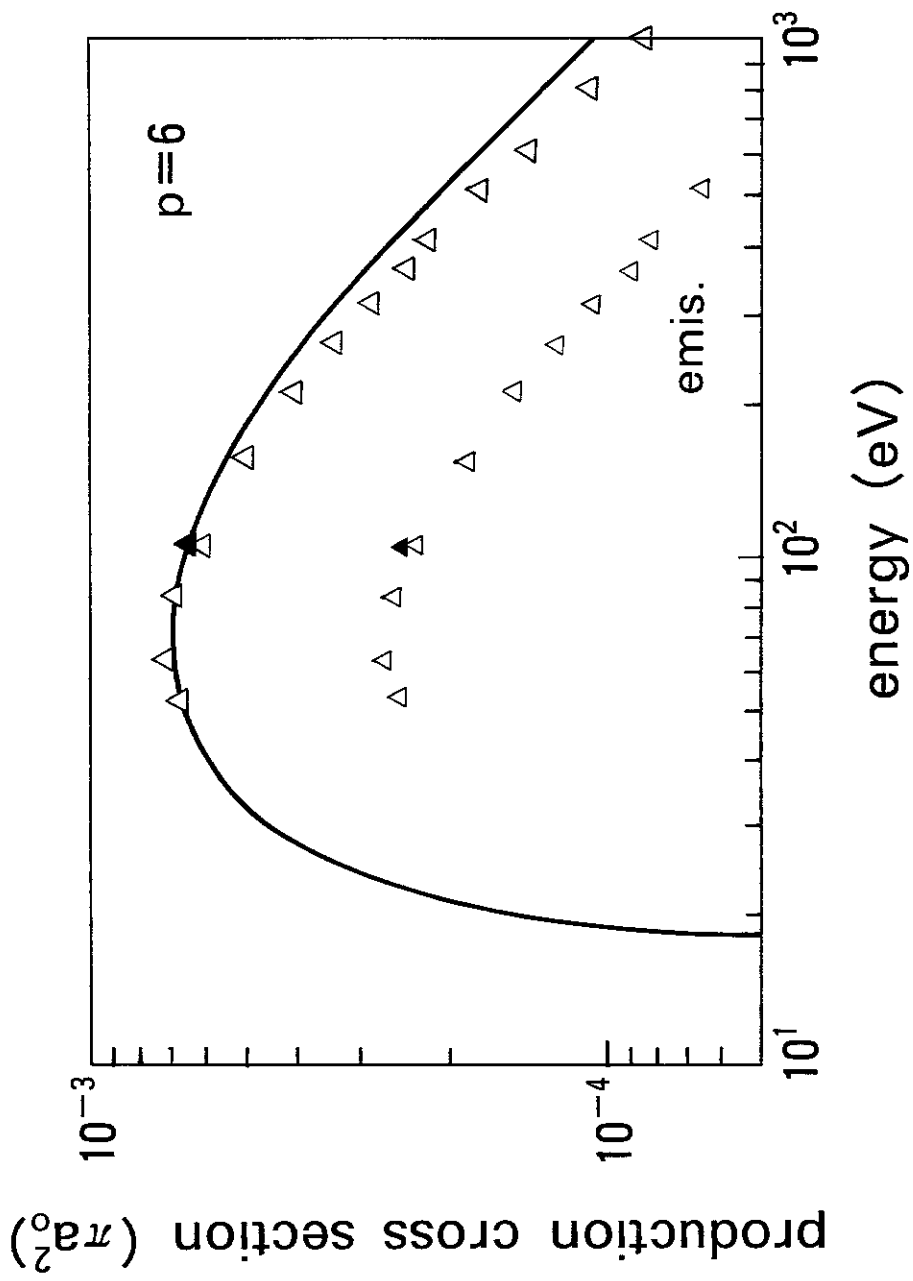


Fig. 5

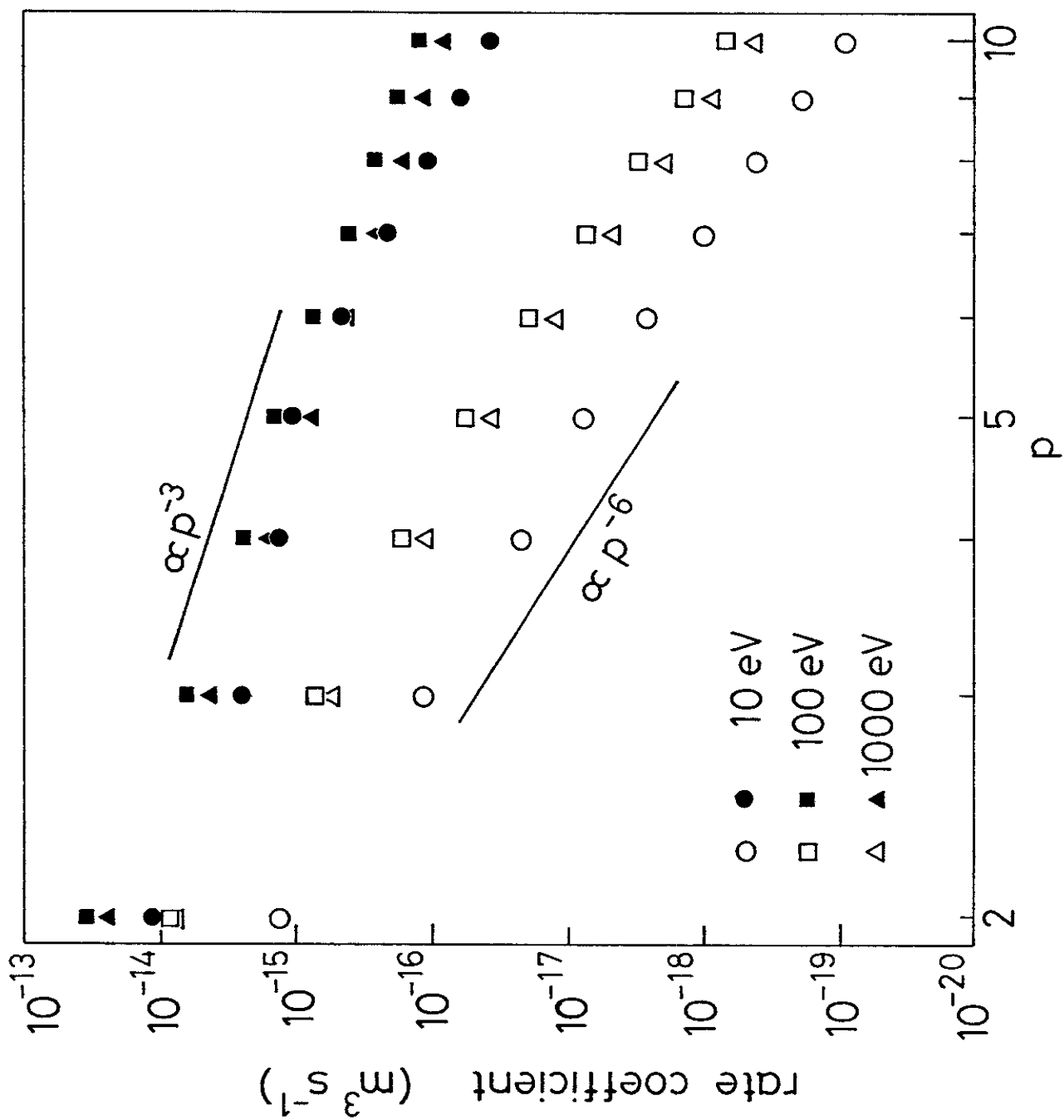


Fig. 6